AMERICAN SOCIETY FOR MICROBIOLOGY | Applied and Environmental Microbiology

Carbon Isotope Fractionation during Catabolism and Anabolism in Acetogenic Bacteria Growing on Different Substrates

Christoph Freude, Martin Blaser

Department of Biogeochemistry, Max-Planck-Institute for Terrestrial Microbiology, Marburg, Germany

Homoacetogenic bacteria are versatile microbes that use the acetyl coenzyme A (acetyl-CoA) pathway to synthesize acetate from CO_2 and hydrogen. Likewise, the acetyl-CoA pathway may be used to incorporate other 1-carbon substrates (e.g., methanol or formate) into acetate or to homoferment monosaccharides completely to acetate. In this study, we analyzed the fractionation of pure acetogenic cultures grown on different carbon substrates. While the fractionation of *Sporomusa sphaeroides* grown on C_1 compounds was strong (ε_{C1}, −49‰ to −64‰), the fractionation of *Moorella thermoacetica* and *Thermoanaerobacter kivui* using glucose ($\varepsilon_{Glu} = -14.1$‰) was roughly one-third as strong, suggesting a contribution of less-depleted acetate from fermentative processes. For *M. thermoacetica*, this could indeed be validated by the addition of nitrate, which inhibited the acetyl-CoA pathway, resulting in fractionation during fermentation ($\varepsilon_{ferm} = -0.4$‰). In addition, we determined the fractionation into microbial biomass of *T. kivui* grown on H_2/CO_2 ($\varepsilon_{anabol.} = -28.6$‰) as well as on glucose ($\varepsilon_{anabol.} = +2.9$‰).

Acetogenic bacteria are a widespread microbial group unified by their ability to use the reductive acetyl coenzyme A (acetyl-CoA) pathway, which allows chemolithoautotrophic growth on hydrogen and carbon dioxide and is the only known pathway that combines carbon dioxide fixation with energy conservation (1–6). Most acetogens can use the reductive acetyl-CoA pathway for autotrophic growth, reducing 2 carbon dioxide molecules with 4 hydrogen molecules to liberate 1 acetate molecule. Under these conditions, CO_2 reduction with H_2 yields a $\Delta G^{o\prime}$ value of −95 kJ/mol. This is barely enough to generate 1 ATP molecule using either a sodium- or a proton-dependent electron motive force (7). On the other hand, the acetyl-CoA pathway can be accompanied by the fermentation of carbon substrates. Under these autotrophic conditions, the energy yield for, e.g., glucose fermentation to 3 acetate molecules is expressed by the equation $\Delta G^{o\prime} = -310.9$ kJ/mol. In contrast to fermentations of glucose by most other anaerobes, which yield only 1 to 3 ATP molecules via substrate-level phosphorylation during glycolysis, acetogens can redirect the reducing equivalents to the reductive acetyl-CoA pathway, allowing the generation of an additional ATP molecule as described above (3, 8).

One approach to evaluating the contributions of different bacterial pathways to certain compound pools in environmental systems is to use the natural abundance of stable carbon isotopes to track the metabolic activity of certain microorganisms in the environment (9, 10): In principle, each metabolic pathway is characterized by a specific preference for a certain carbon isotope (usually the lighter ^{12}C) during catalysis, resulting in a characteristic depletion of ^{13}C between the substrate and the end product. Mathematically, this depletion is characterized by the so-called apparent fractionation factor (α) or enrichment factor (ε); ε is calculated as $10^3(1-\alpha)$. For an A → B reaction, the fractionation factor is defined as $\alpha_{A,B}$ and is calculated as $(\delta^{13}C_A + 10^3)/(\delta^{13}C_B + 10^3)$ (see equation 6) (11).

There are two types of isotope effects: the equilibrium isotope effect and the kinetic isotope effect. In the first case, equilibrium is attained in a closed, mixed system in which a bidirectional reaction occurs. The associated isotope effects are typically small, e.g., the dissolution of inorganic carbon (DIC) in seawater results in unequal isotope distribution between atmospheric CO_2, which is −7.9‰ depleted of ^{13}C, and dissolved bicarbonate (12, 13). In contrast, biological reactions usually display a kinetic isotope effect, which generally discriminates against the heavy isotope, so that the isotopic value of the product is lower than that of the substrate. Biochemical pathways usually consist of a sequence of irreversible or unidirectional reactions that influence the overall fractionation factor to various extents (14–16). Most biochemical reactions that interconvert C_1 compounds have large fractionation effects; in contrast, most heterotrophic reactions involving complex organic substrates have small fractionation effects (see below). Usually, the fractionation factors are determined in pure microbial cultures and can be derived from either substrate depletion or product accumulation (17). A well-documented example of carbon isotope fractionations is methanogenesis from different substrates: fractionation factors are −25‰ to −69‰ with CO_2 (18–21), −73‰ to −83‰ with methanol (22, 23), and −7‰ to −35‰ with acetate (21, 24–27). In environmental samples, fractionation factors can be used to distinguish different pathways if the difference in fractionation is large enough. For example, the fractionation factor for hydrogenotrophic methanogenesis can be determined by the incubation of soil samples in the presence of CH_3F (28–31), which specifically inhibits acetoclastic methanogenesis (32, 33).

The acetyl-CoA pathway imparts strong isotopic enrichment of −55‰ to −60‰ during acetate formation with H_2/CO_2 (80/

Received 27 October 2015 **Accepted** 21 February 2016

Accepted manuscript posted online 26 February 2016

Citation Freude C, Blaser M. 2016. Carbon isotope fractionation during catabolism and anabolism in acetogenic bacteria growing on different substrates. Appl Environ Microbiol 82:2728–2737. doi:10.1128/AEM.03502-15.

Editor: A. J. M. Stams, Wageningen University

Address correspondence to Martin Blaser, blaserm@mpi-marburg.mpg.de.

Supplemental material for this article may be found at http://dx.doi.org/10.1128/AEM.03502-15.

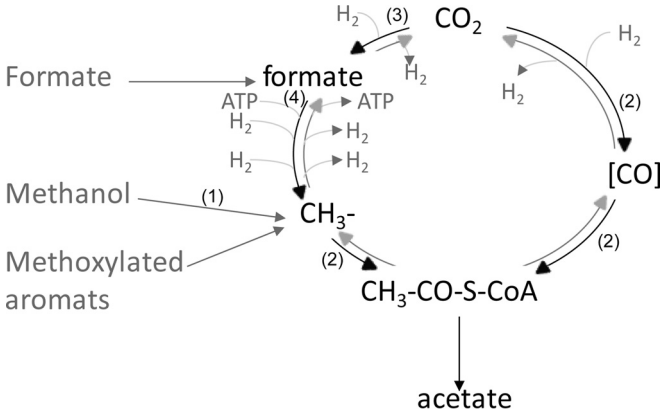

FIG 1 Schematic representation of the reductive acetyl-CoA pathway and entry points of possible substrates. The reduction of CO_2 to either the methyl or the carboxyl group is shown in black; the reverse reaction (oxidation) is shown in gray. For simplicity, reducing equivalents are given as H_2. The entry points of different C_1 substrates are shown in dark gray. Note that the carboxyl group can be formed by the reduction of CO_2 or indirectly, by the oxidation of the respective C_1 compound. Numbers in parentheses represent the enzymes acting on the different C_1 compounds, as follows: 1, methanol-cobalamin methyltransferase; 2, CO dehydrogenase/acetyl-CoA synthase; 3, formate dehydrogenase; 4, formyl-tetrahydrofolate synthetase. Details on the reactions are given in equations 1 to 6 and in the text.

20) as the substrate (34–36). In contrast, the fractionation associated with acetate fermentation by microbial glycolytic fermentation is weak (<5‰) (37–40).

However, the fractionation of the reductive acetyl-CoA pathway used by acetogenic bacteria has so far been evaluated only for pure cultures grown on H_2/CO_2. As shown in Fig. 1, in this pathway, 1 CO_2 molecule is fixed by formate dehydrogenase and is then reduced stepwise to the methyl group of acetate (methyl branch), while a second molecule of CO_2 is directly used by the CO dehydrogenase/acetyl-CoA synthase (CODH/ACS) to form the carboxy group of acetate (carbonyl branch) (41, 42). It has been shown that both branches exhibit the same strong fractionation when H_2/CO_2 is used as a substrate (35).

We hypothesized that other C_1 compounds that can be incorporated either alone or in the presence of H_2/CO_2 may affect the overall fractionation of the resulting acetate. In this study, we tested two substrates (formate and methanol) entering at different sites of the methyl branch. In addition, we grew *Thermoanaerobacter kivui* mixotrophically on H_2/CO_2 together with different formate concentrations.

In a second project, we evaluated the fractionation of pure acetogenic cultures during fermentation. As a model substrate, we used glucose, which is oxidized by many acetogens to 2 pyruvate molecules via glycolysis and is then oxidatively decarboxylated to acetyl-CoA. The reducing equivalents and the CO_2 released are used by the reductive acetyl-CoA pathway to generate a third molecule of acetate (1, 3, 8, 43). Therefore, we expect that two-thirds of the acetate released originates from the oxidative decarboxylation of pyruvate and the remaining one-third from the acetyl-CoA pathway. This suggests that the $\delta^{13}C$ value is affected by both pathways and is a combination of the weak fractionation (<5‰) during glycolysis and oxidative decarboxylation (37–40) and the strong fractionation (−38‰ to −68‰) caused by the acetyl-CoA pathway (34–36). To further test the contribution of each reaction, we added nitrate as an alternative electron acceptor, since nitrate can be used by some acetogens instead of the acetyl-CoA pathway to deplete the reducing equivalents produced by glycolysis (44–46). From these incubations, we can estimate the isotopic contribution of the acetate originating from pyruvate decarboxylation alone.

As a third objective, we evaluated the fractionation of acetogenic bacteria during anabolism. Usually, calculations of the fractionation factor rely on a mass balance equation focusing on the catabolic processes and neglecting the anabolic reactions. Since we observed a higher optical density for *T. kivui* when it was grown on glucose than when it was grown on H_2/CO_2, we wondered if the fractionation during anabolic reactions could be neglected for the calculations of stable carbon isotope fractionation. So far, the fractionation into biomass has been determined mainly at the end of incubation for several CO_2-fixing pathways (26, 47, 48) and in methanogens grown on different substrates (22) and at several time points during aerobic mineralization of 1,2-dichloroethane by *Xanthobacter autotrophicus* as reported by Hunkeler and Aravena (49). In all cases, the isotopic signal of anabolism was lower than the fractionation during catabolism. We hypothesized, therefore, that the fractionation of pure acetogenic cultures into biomass would be lower than the fractionation into acetate. In contrast to the procedures in most previous studies, we performed a time series experiment, which allows precise calculation of the fractionation factors during anabolism and catabolism.

Altogether, we intended to estimate how strongly the fractionation of stable carbon isotopes associated with the acetyl-CoA pathway is affected by the substrate usage of pure acetogenic cultures.

MATERIALS AND METHODS

Growth conditions. *Moorella thermoacetica* DSM 2995, *Sporomusa sphaeroides* DSM 2875, and *Thermoanaerobacter kivui* DSM 2030 were obtained from the Deutsche Sammlung von Mikroorganismen und Zellkulturen (Braunschweig, Germany). The cultures were grown at 55°C (*M. thermoacetica*, *T. kivui*) or 30°C (*S. sphaeroides*). The medium contained the following (per liter): $NaHCO_3$, 7.5 g; K_2HPO_4, 0.22 g; KH_2PO_4, 0.22 g; NH_4Cl, 0.31 g; $(NH_4)_2SO_4$, 0.22 g; NaCl, 0.45 g; $MgSO_4 \cdot 7H_2O$, 0.09 g; cysteine, 0.5 g; $Na_2S \cdot 9H_2O$, 0.5 g; $NH_4Fe(SO_4)_2$, 10 mg; resazurin, 0.5 mg. A trace element solution (10 ml per liter) and a vitamin solution (5 ml per liter) (50) were added. The trace element solution consisted of the following (per liter): nitrilotriacetic acid, 1.5 g; $MgSO_4 \cdot 7H_2O$, 3 g; $MnSO_4 \cdot H_2O$, 0.5 g; NaCl, 1 g; $FeSO_4 \cdot 7H_2O$, 0.1 g; $CoSO_4 \cdot 7H_2O$, 0.18 g; $CaCl_2 \cdot 2H_2O$, 0.1 g; $ZnSO_4 \cdot 7H_2O$, 0.18 g; $CuSO_4 \cdot 5H_2O$, 0.01 g; $KAl(SO_4)_2 \cdot 12H_2O$, 0.02 g; H_3BO_3, 0.01 g; $Na_2MoO_4 \cdot 2H_2O$, 0.01 g; $NiCl_2 \cdot 6H_2O$, 0.025 g; $NaSeO_3 \cdot 5H_2O$, 0.3 mg (pH 7.0).

The cultures were routinely grown in the minimal medium described in the previous paragraph with the addition of a defined carbon source (glucose, fructose, or betaine) under N_2/CO_2 (80:20). For the experiments, 100 μl of these precultures was inoculated in the same minimal medium containing filter-sterilized (pore size, 0.2 μm) stock solutions of the respective substrate: glucose (final concentration, 5 mM), methanol (final concentration, 20 mM), or formate (final concentration, 5 or 20 mM). For the chemolithotrophic experiments, the same minimal medium lacking a carbon source was used under a headspace of H_2/CO_2 (80:20). The reactions for the different substrates (compare Fig. 1) are as follows:

$$4H_2 + 2CO_2 \Rightarrow 1CH_3COOH + 2H_2O \quad (1)$$

$$4HCOOH \Rightarrow 1CH_3COOH + 2CO_2 + 2H_2O \quad (2)$$

$$1HCCOH + 3H_2 + CO_2 \Rightarrow 1CH_3COOH + 2H_2O \quad (3)$$

$$4CH_3OH + 2CO_2 \Rightarrow 3CH_3COOH + 2H_2O \quad (4)$$

$$1C_6H_{12}O_6 \Rightarrow 3CH_3COOH \quad (5)$$

Cultures were grown in 120-ml serum bottles, which contained 50 ml medium. At the times indicated in the figures, 100-μl gas samples were taken with a gastight syringe (Vici, Baton Rouge, LA, USA) for analysis of the concentrations and $\delta^{13}C$ values of both CO_2 and CH_4; 2-ml liquid samples were taken for analysis of the concentrations and $\delta^{13}C$ values of glucose and short-chain fatty acids (SCFA).

Chemical and isotopic analyses. CH_4 was analyzed by gas chromatography (GC) using a flame ionization detector (Shimadzu, Kyoto, Japan). CO_2 was analyzed after conversion to CH_4 with a methanizer (Ni catalyst at 350°C; Chrompack, Middelburg, Netherlands). Isotope ratio ($^{13}C/^{12}C$) measurements in gas samples were performed on a gas chromatography combustion isotope ratio mass spectrometer (GC-C–IRMS) system (Thermo Fisher Scientific, Bremen, Germany). The principle of operation has been described by Brand (51). The gaseous compounds were first separated in a Hewlett-Packard 6890 GC using a PoraPLOT Q column (length, 27.5 m; internal diameter, 0.32 mm; film thickness, 10 μm; Chrompack, Frankfurt, Germany) at 30°C with He (purity, 99.996%; 2.6 ml/min) as the carrier gas. The sample was run through the Finnigan Standard GC Combustion Interface III, and the $^{13}C/^{12}C$ isotope ratio was analyzed in the IRMS (Finnigan MAT Delta Plus). The reference gas was CO_2 (purity, 99.998%) (Air Liquide, Düsseldorf, Germany), calibrated with the working standard methyl stearate (Merck). The latter was intercalibrated at the Max Planck Institute for Biogeochemistry, Jena, Germany (courtesy of W. A. Brand) against the NBS-22 and USGS-24 standards, and the stable carbon isotope ratio was measured against that of Vienna Pee Dee Belemnite and is reported in the delta notation as follows:

$$\delta^{13}C = 10^3\left(R_{sample}/R_{standard} - 1\right) \quad (6)$$

where R is the $^{13}C/^{12}C$ ratio.

Isotopic analysis and quantification of glucose and SCFA were performed on a high-pressure liquid chromatography (HPLC) system (SpectraSYSTEM P1000; Thermo Fisher Scientific, San Jose, CA, USA) with a Mistral thermostat (Spark, Emmen, Netherlands), equipped with an ion exclusion column (Aminex HPX-87H; Bio-Rad, Munich, Germany) and coupled to the Finnigan LC IsoLink interface (Thermo Fisher Scientific, Bremen, Germany) as described previously (52). Isotope ratios were detected on an IRMS (Finnigan MAT Delta Plus Advantage). The precision of the GC-IRMS was ±0.2‰, and that of the HPLC-IRMS was ±0.3‰. For further details on the determination of acetate concentrations via HPLC-IRMS, see Fig. S9 and Table S2 in the supplemental material.

The isotopic fractionation into biomass was evaluated by harvesting three replicate samples (120-ml serum bottles), each containing 50 ml of culture, for each time point. The cells were harvested by centrifugation (10 min at 6,000 rpm [9,700 × *g*]). The resulting pellet was dried in tin capsules and was sent to the isotope center in Göttingen, Germany. There the isotopic values were determined using an elemental analyzer coupled to an IRMS (Kompetenzzentrum Stabile Isotope, University of Göttingen). Pure acetate was used as a reference to compare our HPLC-IRMS measurement with the results of the elemental analyzer.

Calculations. The apparent fractionation factor (α) for an A → B reaction is defined according to reference 11 as

$$\alpha_{A/B} = \left(\delta_A + 1,000\right)/\left(\delta_B + 1,000\right) \quad (7)$$

and the isotope enrichment factor is defined as $\varepsilon = 10^3(1 - \alpha)$. The isotope enrichment factor associated with homoacetogenesis was determined as described by Mariotti et al. (17) from the residual reactant

$$\delta_r = \delta_{ri} + \varepsilon\left[\ln\left(1 - f\right)\right] \quad (8)$$

and from the product formed

$$\delta_p = \delta_{ri} - \varepsilon\left(1 - f\right)\left[\ln\left(1 - f\right)\right]/f \quad (9)$$

where δ_{ri} is the isotope composition of the reactant (CO_2) at the beginning, and δ_r and δ_p are the isotope compositions of the residual CO_2 and the pooled acetate, respectively, at the instant when f was determined. Linear regression of δ_r against $\ln(1 - f)$ and linear regression of δ_p against $(1 - f)[\ln(1 - f)]/f$ give ε as the slope of best-fit lines. The fractional yield of a reaction (f) is usually based on the consumption of the substrate CO_2 ($0 < f < 1$); in a closed system, the amount of substrate used (f_{delta}) can be derived from the measured isotopic composition (35) as follows:

$$f_{delta} = \left(\delta_{ri} - \delta_r\right)/\left(\delta_p - \delta_r\right) \quad (10)$$

In contrast to the isotope enrichment factor (ε) derived from pure microbial cultures as described above, many environmental studies calculate the environmental fractionation (Δ) as follows:

$$\Delta = \delta_{prod} - \delta_{subst} \quad (11)$$

where δ_{subst} is the $\delta^{13}C$ value of the substrate and δ_{prod} is the $\delta^{13}C$ value of the product.

While this estimated fractionation is valid for open systems, such as environmental samples, it is valid in a closed system with limited substrate concentrations only at the very beginning of a reaction (17, 53, 54). Nevertheless, we used this formula for the mixotrophic experiments to estimate the environmental fractionation into acetate versus biomass for cells grown on formate or H_2/CO_2.

RESULTS

Growth on C_1 compounds. In order to evaluate the fractionation factor in the acetyl-CoA pathway, we measured the production of acetate during the consumption of different C_1 compounds that either are direct intermediates (CO_2, formate) or can be easily incorporated into the acetyl-CoA pathway (methanol) (Fig. 1). These experiments were conducted using *Sporomusa sphaeroides*. Substrate depletion and product formation were analyzed over time, and the $\delta^{13}C$ values of all carbon-containing compounds were measured during the reaction (Fig. 2). Despite the different ^{13}C values of the initial substrates methanol ($\delta_{methanol} = -38‰$), formate ($\delta_{formate} = -31‰$), and H_2/CO_2 ($\delta_{CO2} = -17‰$), the acetate released with all three substrates eventually reached the same value ($\delta_{acetate} = -67‰$). The $\delta^{13}C$ values of all three substrates became enriched in heavy carbon at roughly the same rate. When the apparent fractionation factors were calculated on the basis of the substrate data, the ε values obtained were −56.9‰ for methanol, −56.5‰ for formate, and −63.8‰ for CO_2 (with H_2/CO_2 as the substrate). The $\delta^{13}C$ of CO_2 did not differ much whether methanol or formate served as the substrate, due to the high background level of bicarbonate (4.5 mmol $NaHCO_3$/bottle) in the culture medium. Details on acetate formation for the individual substrates are given in Fig. S2 in the supplemental material. Details and further discussion of the isotope values of acetate are given in Fig. S3 and the accompanying discussion in the supplemental material.

In a different approach, the influence of different C_1 compounds was tested using the thermophilic acetogen *Thermoanaerobacter kivui* grown under a headspace of N_2/CO_2 on formate (1 mmol per bottle). In parallel, *T. kivui* was inoculated under a headspace of H_2/CO_2 (2.5 mmol H_2 and 0.6 mmol CO_2 per bottle [70 ml headspace in 120 ml]) either alone or under mixotrophic conditions in the presence of a low (0.25 mmol per bottle [50 ml medium per 120-ml bottle]) or a high (1 mmol per bottle [50 ml medium per 120-ml bottle]) concentration of formate (Fig. 3; Table 1). The bicarbonate concentration was 4.5 mmol per bottle in all incubations. Details on carbon turnover are given in Fig. S4 in the supplemental material. Using hydrogen consumption (equation 1) and formate consumption (equation 3) as proxies for

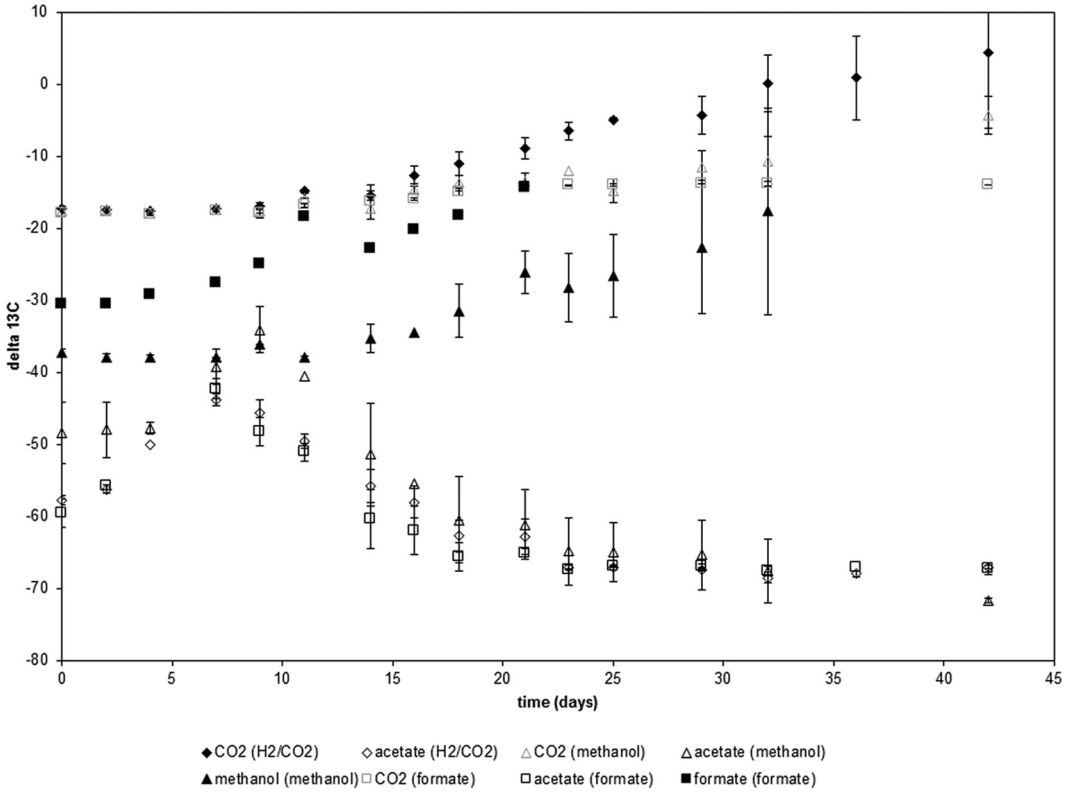

FIG 2 *Sporomusa sphaeroides* DSM 2875 grown on different C_1 compounds. (The substrate [H_2/CO_2, formate, or methanol] is given in parentheses in the key after the analyte measured.) Shown are the $\delta^{13}C$ values of the substrate (filled symbols) and the product (acetate) (open symbols); $\delta^{13}C$ values of CO_2 for incubations with methanol or formate are represented by open symbols with gray borders. Values are averages for three independent replicates ± standard deviations. Individual plots for the different substrates are given in Fig. S1 in the supplemental material.

substrate turnover into acetate, almost-complete turnover could be documented for all experiments (Table 1). This substrate consumption was used to calculate the relative contributions of the two substrates under mixotrophic conditions and to estimate the apparent fractionation (Δ) between the substrate (at time zero [t_0]) and the product, acetate (at the end of the reaction [t_{end}]), or between the substrate (at t_0) and biomass (at t_{end}). A statistically nonsignificant trend toward ^{13}C depletion of acetate as well as biomass could be observed for increasing contributions of formate relative to CO_2 (Table 1). Calculation of enrichment factors using the linear regression given in equation 8 gave a ε_{CO2} of −48.7‰ for incubations under H_2/CO_2 and a ε_{form} of −51.9‰ for formate incubations under N_2/CO_2.

Growth on glucose and nitrate inhibition. In a further set of experiments, fractionation was determined when pure acetogenic cultures were grown on complex carbon substrates. As an example, *Moorella thermoacetica* grown on glucose alone (200 μmol), glucose (200 μmol) plus nitrate (300 μmol), or H_2/CO_2 (2.5 mmol/625 μmol) was used. Indeed, our isotopic measurements revealed almost no fractionation with glucose and nitrate ($\varepsilon_{Glu+NO3}$ = −0.4‰), strong fractionation with H_2/CO_2 ($\varepsilon_{H2/CO2}$ = −55.8‰), and intermediate fractionation with glucose (ε_{Glu} = −18.5‰), reflecting the mixing of the two acetate-generating pathways (Fig. 4). Additional data on nitrate depletion are given in Fig. S5 in the supplemental material. Similar results could be obtained for *T. kivui*, where the fractionation under glucose (ε_{Glu} = −14.1‰) was roughly one-third of the fractionation under H_2/CO_2 ($\varepsilon_{H2/CO2}$ = −53.0‰) (see Fig. S6 in the supplemental material), and also for *Acetobacterium carbinolicum* (ε_{Glu} = −18.8‰; $\varepsilon_{H2/CO2}$ = −54.0‰) (data not shown).

Fractionation into biomass. In contrast to aerobic bacteria, anaerobic bacteria can use only a small amount of the available energy for anabolism (usually around 10%), and hence only a small portion of the available carbon is fixed into biomass. However, it was observed that *T. kivui* grew to dense cultures on glucose, but only faint turbidity was observed for cells grown on H_2/CO_2. Therefore, we questioned how substrate usage affects the $\delta^{13}C$ values of the microbial biomass. *Thermoanaerobacter kivui* was grown on glucose (200 μmol under N_2/CO_2) or on H_2/CO_2 (2.5 mmol/625 μmol) in the bicarbonate-buffered minimal medium described above. We expected that under these two conditions, roughly the same amount of acetate would be produced. The $\delta^{13}C$ values of the substrates and the product, as well as those of biomass, were followed over time (Fig. 5). The fractionation during catabolism was calculated with equation 8 using the ^{13}C values of the substrate together with the ^{13}C values of acetate; the fractionation during anabolism was calculated using the ^{13}C values of the substrate together with the ^{13}C values of the biomass. While growth on glucose resulted in weak positive fractionation during catabolism ($\varepsilon_{catabol.}$ = +4.2‰) as well as during anabolism ($\varepsilon_{anabol.}$ = +2.9‰), growth on H_2/CO_2 was accompanied by stronger fractionation during catabolism ($\varepsilon_{catabol.}$ = −48.6‰) than during anabolism ($\varepsilon_{anabol.}$ = −28.6‰).

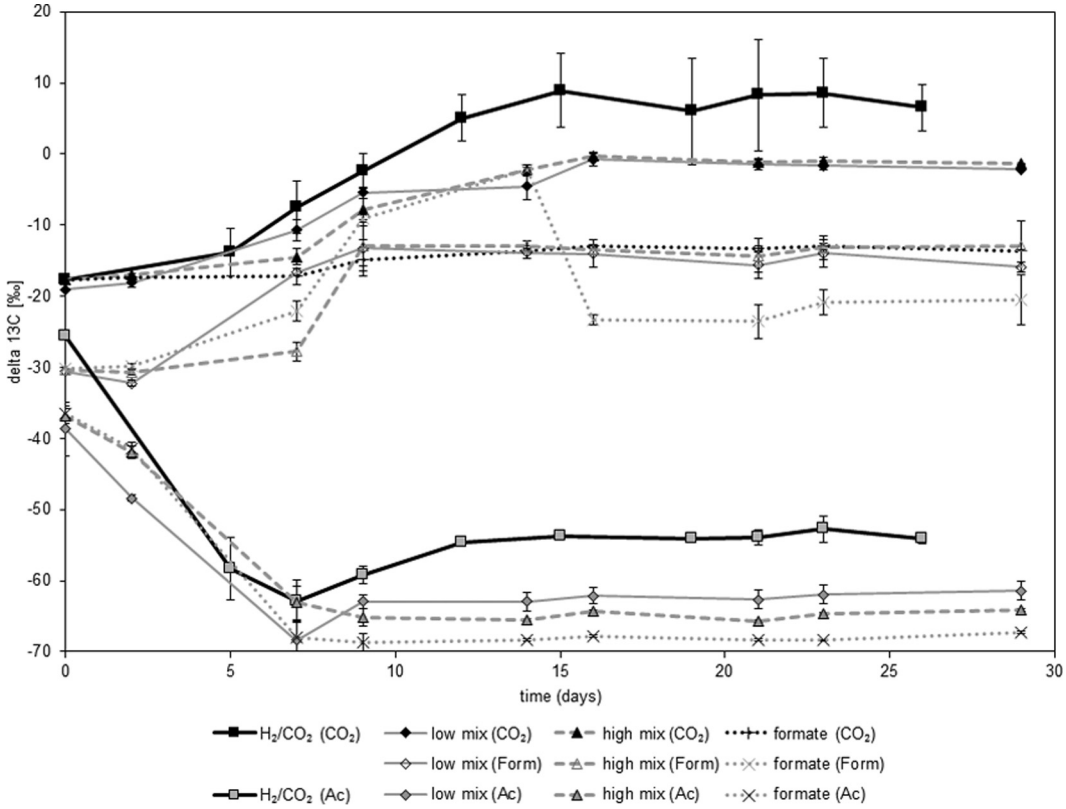

FIG 3 Mixotrophic growth of *Thermoanaerobacter kivui* DSM 2030 on formate and H_2/CO_2 leads to the incorporation of both substrates. The analytes measured—CO_2, formate (Form), and acetate (Ac)—are given in parentheses in the key. H_2/CO_2 concentrations were 2.5 mmol/bottle (H_2) and 0.6 mmol/bottle (CO_2) in the H_2/CO_2 treatment as well as in the low- and high-mix treatments (incubations in the presence of a low or a high concentration of formate, respectively, under a headspace of H_2CO_2). Formate concentrations were 0.25 mmol/bottle in the low-mix treatment and 1 mmol/bottle in the high-mix and formate treatments. The $\delta^{13}C$ value of the released acetate is a direct result of the mixing of the $\delta^{13}C$ values of the substrates, while the fractionation of the individual substrates is quite constant. Values are averages for three independent replicates ± standard deviations.

DISCUSSION

Growth on C_1 compounds. The data presented in this report confirmed the overall strong fractionation of acetogens using the acetyl-CoA pathway when H_2/CO_2 was the substrate (34, 35); in addition, it could be shown that the fractionation of cells grown on different C_1 compounds likewise resulted in very strong fractionation and was largely independent of substrate usage (different C_1 compounds). This is in contrast to the findings of several published reports where the rate-limiting step (usually the initial step of a reaction cascade) primarily determined the overall fractionation (20–23, 25, 27, 55, 58).

One prominent example of the initial step of a reaction cascade determining the overall fractionation can be found in plant systems, where the initial CO_2-fixing reactions of C_3 and C_4 plants (RubisCO versus phosphoenolpyruvate carboxylase) dictate strong differences in the resulting plant material (55), a pattern that is largely unchanged throughout the food chain (56, 57). In the microbial world, similar behavior is well documented for pure

TABLE 1 Mixotrophic growth of *T. kivui* on H_2/CO_2 and different amounts of formate

Substrate[a]	Amt (mmol/bottle) of:			Recovery (%)[b]	% of acetate from H_2[c]	$\delta^{13}C$ (‰)				Apparent fractionation[d]	
	Formate used	H_2 used	Acetate formed			Formate (t_0)	CO_2 (t_0)	Acetate (t_{end})	Biomass (t_{end})	$\Delta_{substrate\text{-}acetate}$	$\Delta_{substrate\text{-}biomass}$
H_2/CO_2		1.9	0.5	95	100		−17.7	−54.2	−27.9	−36.5	−10.2
Low mix	0.3	2.1	0.7	93	80	−30.6	−19.1	−61.4	−34.0	−40.0	−12.6
High mix	1.1	2.1	0.8	102	53	−30.4	−17.7	−64.1	−38.4	−40.4	−14.7
Formate	1.2		0.3	108	0	−30.2	−17.6	−67.3	−47.1	−37.1	−17.1

[a] Low mix, H_2/CO_2 and a low concentration of formate; high mix, H_2/CO_2 and a high concentration of formate.
[b] Calculated using equations 1 and 3 and assuming substrate limitation (either H_2 or formate). Since the cells were grown in a bicarbonate-buffered system (4.5 mmol $NaHCO_3$/bottle), CO_2 was never limiting.
[c] The percentages of acetate from H_2 have been calculated assuming complete turnover of H_2 and formate into acetate using the reactions given in equations 1 and 3.
[d] Derived from the $\delta^{13}C$ values of the substrate and product assuming the percentages of acetate from H_2 given in this table.

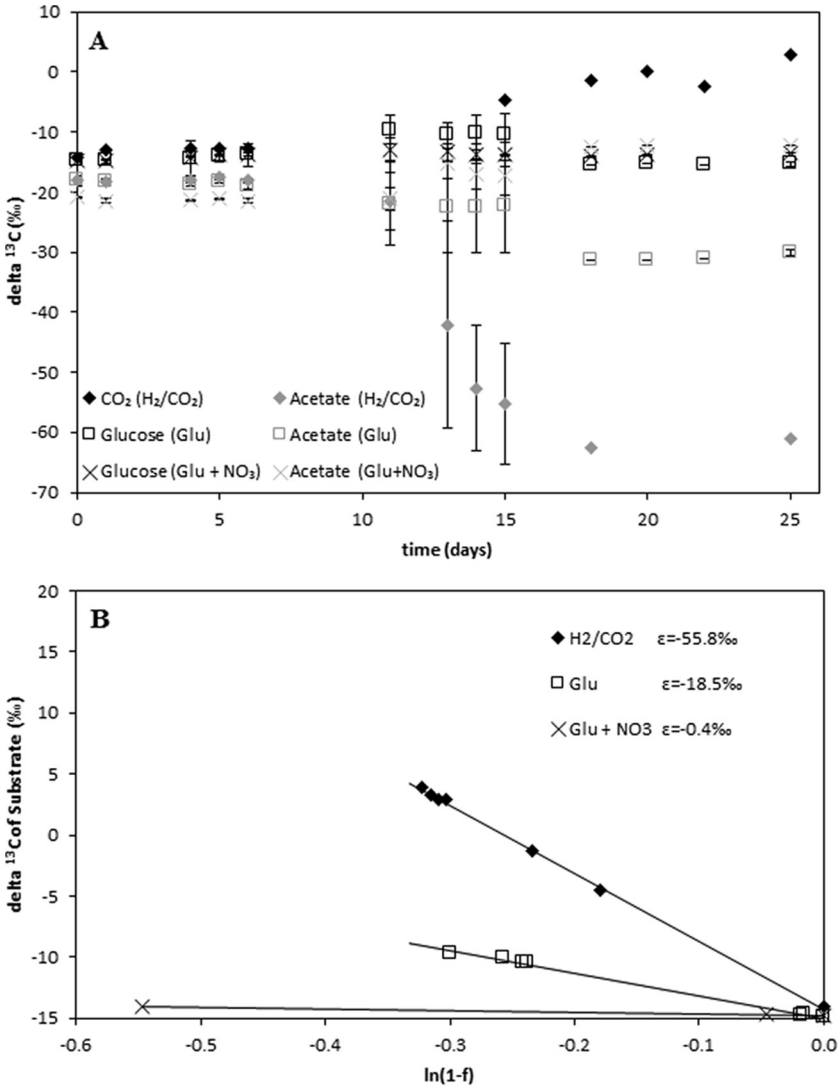

FIG 4 *Moorella thermoacetica* DSM 2955 grown on H_2/CO_2 (◆), glucose alone (□), or glucose with nitrate (×). (A) $\delta^{13}C$ values of the substrate (CO_2 or glucose) and the product (acetate). In the key, the different treatments—H_2/CO_2, glucose (Glu), and glucose plus nitrate (Glu + NO_3)—are given in parentheses. (B) Regression analysis of the respective incubations. The $\delta^{13}C$ value of acetate reflects the stoichiometry of the producing pathway. For example, on glucose, two-thirds of the acetate released originates from glycolysis and decarboxylation ($\varepsilon_{Glu+NO3} = -0.4‰$) and one-third from the acetyl-CoA pathway ($\varepsilon_{H2/CO2} = -55.8‰$); the coordinated action of both pathways results in a mixed fractionation reflecting the contribution of each ($\varepsilon = -18.5‰$).

methanogenic cultures on different substrates, where each substrate is accompanied by a unique fractionation factor. For example, pure methanogenic cultures of *Methanosarcina barkeri* grown on different carbon substrates show highly distinct carbon isotope fractionations between substrate and product when grown on H_2/CO_2 (−45.4‰ to −46.3‰), methanol (−72.5‰ to −83.4‰), or acetate (−21.2‰ to −34.8‰) (22, 58). These results have been independently validated for other pure methanogenic cultures on H_2/CO_2 (20, 21), methanol (23), and acetate (25, 27). Further, it was shown for hydrogenotrophic methanogens (using H_2/CO_2) that fractionation is greatly affected by the hydrogen (energy) level of the incubation, with stronger fractionation under H_2-limiting conditions (20–22). For a sulfate-reducing *Desulfovibrio* sp., the fractionation of sulfur isotopes was also affected by the electron donors and was negatively correlated with the cell-specific sulfate reduction rate (59). Recent evidence also suggests that for sulfate-reducing bacteria, the overall isotope fractionation during sulfate reduction is influenced by all steps in the dissimilatory pathway (16, 60).

In contrast, differences in the substrate ratios of H_2 and CO_2 for acetogenic cultures did not affect fractionation (61). Furthermore, it has been shown that there is no intramolecular fractionation during acetate formation: the isotope values of the methyl group were similar to the $\delta^{13}C$ values of the overall acetate signal (35). The range of fractionations for different C_1 compounds reported in this study is well within the range reported previously (−38‰ to −68‰) for acetogenic cultures grown on H_2/CO_2 (34, 35). And now our data on the conversion of different C_1 compounds to acetate suggest similar discrimination against ^{13}C irrespective of the individual C_1 compound.

Our results for the *S. sphaeroides* incubations can be interpreted in two ways. (i) One explanation is that the initial fraction-

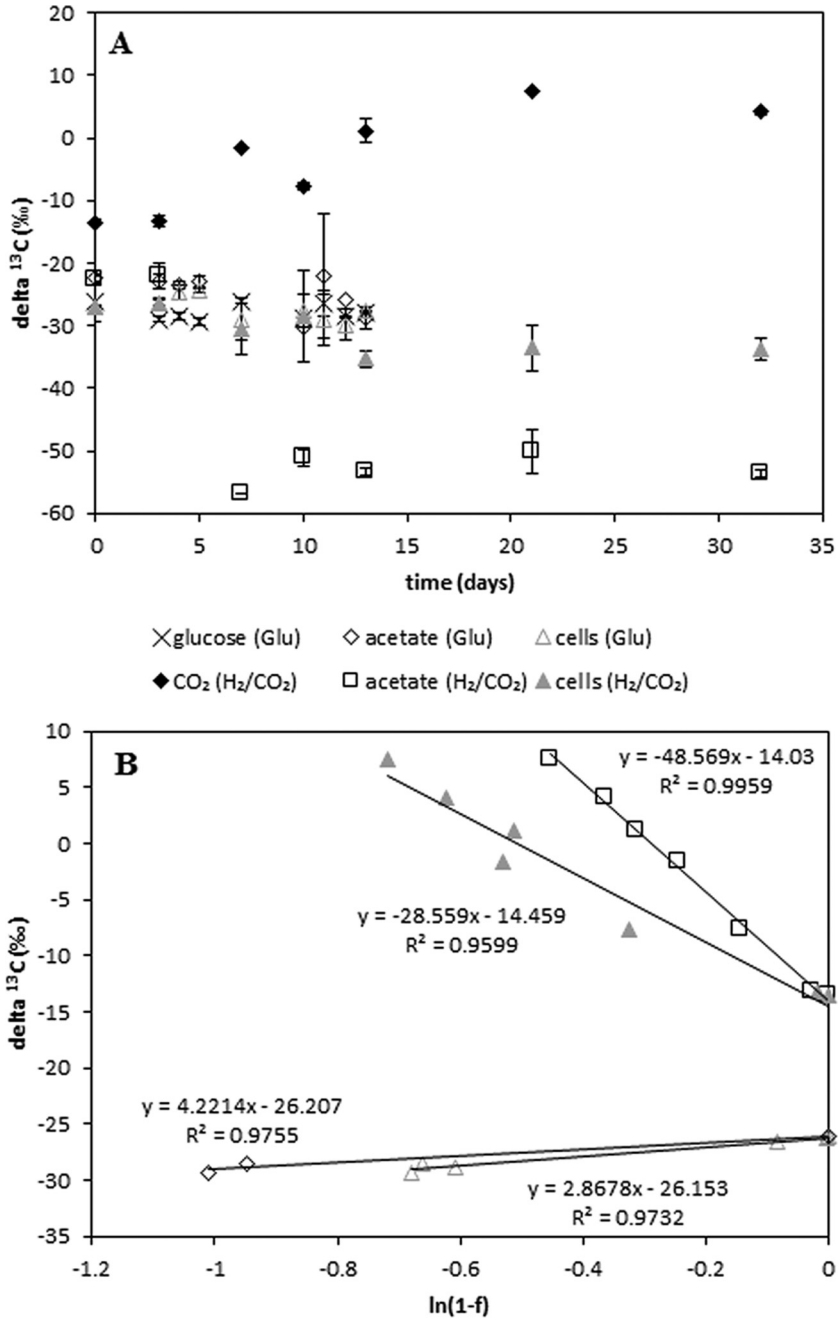

FIG 5 Fractionation into biomass. (A) $\delta^{13}C$ values for *Thermoanaerobacter kivui* grown on either H_2/CO_2 or glucose. Three replicate samples were harvested for each time point. In the key, the substrates are given in parentheses. (B) Regression analysis of CO_2 conversion into acetate □ or biomass △ for cells grown on H_2/CO_2 and regression analysis of glucose conversion into acetate ◇ or biomass △ for cells grown on glucose.

ations of all possible initial enzymes are highly similar. (ii) Alternatively, our results can be explained by assuming that the rate-limiting step determining overall fractionation is the formation of a C—C bond by the CODH/ACS complex. We will discuss both possibilities:

(i) The individual entry points for the different C_1 compounds are schematically given in Fig. 1. The following four enzymes are involved: methanol-cobalamin methyltransferase, CO dehydrogenase/acetyl-CoA synthase, formate dehydrogenase, and formyl-tetrahydrofolate synthetase. Methanol is incorporated using methanol-cobalamin methyltransferase (62). While 1 molecule of CO_2 is reduced via CO to the carboxyl group of acetate by the enzyme complex CO dehydrogenase/acetyl-CoA synthase, a second molecule of CO_2 is reduced to formate by formate dehydrogenase. Hence, formate is a direct intermediate and can be either oxidized to CO_2 or further reduced in an ATP-dependent reaction catalyzed by formyl-tetrahydrofolate synthetase (3). In principle, it is possible that all four of these entry points could exhibit the same fractionation. However, fractionation of methanol and CO_2 in pure methanogenic cultures renders completely different frac-

tionation factors when homologous enzymes are used for the initial incorporation. Therefore, we think that in acetogenic bacteria, fractionation is controlled mainly by a later step in the reductive acetyl-CoA pathway, presumably the condensation of the 2 carbon molecules in the CODH/ACS system:

(ii) All the substrates we used were incorporated into the methyl branch of the acetyl-CoA pathway (Fig. 1), yielding the methyl group of the released acetate. However, the reduction of formate is accompanied by the release of CO_2 (equation 2); while one part of the methanol is oxidized to CO_2 to provide reducing equivalents, 3 molecules of methanol and 3 molecules of CO_2 are reduced to 3 molecules of acetate, resulting in a net consumption of 2 molecules of CO_2 (equation 4). In any case, our experimental setup does not allow us to determine whether the carboxyl group is directly formed from external CO_2 reduction (e.g., carbonate buffer) or originates from an intracellular CO_2 pool generated through the oxidation of methanol or formate.

The acetyl-CoA pathway can operate in both directions; while most acetogens use it for carbon fixation from CO_2 and energy conservation via an Ech or Rnf system (7), others can operate in the reverse direction together with a syntrophic partner to perform syntrophic acetate oxidation (63, 64). As a result, most reactions of the acetyl-CoA pathway can be seen as highly reversible and hence can easily equilibrate different isotopic $\delta^{13}C$ values. Therefore, it is plausible that the first condensing step, not the initial step, is the critical point for fractionation. Indeed, this explanation would be in agreement with the results obtained for the C_3 and C_4 plants, where the initial step is a C—C-forming condensation reaction.

When *T. kivui* is grown at the expense of a methylated aromatic compound (vanillic acid), the initial step (O-demethylation of vanillic acid) may be less reversible. Indeed, initial trials resulted in less depleted acetate for *T. kivui* grown at the expense of vanillic acid ($\delta_{ac} = -50‰$) (see Fig. S7 in the supplemental material) than for cultures grown on C_1 compounds ($\delta_{ac} = -67‰$) (Fig. 1). These data could not be further evaluated, however, since the ^{13}C value of the substrate vanillic acid could not be measured using our HPLC-IRMS approach.

Growth on glucose and nitrate inhibition. Both cultures investigated (*M. thermoacetica* and *T. kivui*) showed strong fractionation (ca. −50‰ to −55‰) during acetate formation when the acetyl-CoA pathway was the only operative pathway (34). As soon as glucose was used as a substrate, the apparent fractionation was due to a mixture of fermentation and the acetyl-CoA pathway and was less than −20‰.

These findings have environmental implications. The strong fractionation during acetate production via the acetyl-CoA pathway can easily be tracked in natural environments. Ideally, it can be used to estimate the contribution of acetogens to the acetate pool when the fractionations of all other acetate-generating and -depleting reactions are known (9). The mixed fractionation of acetogens grown on molecules larger than C_1, such as glucose (less than −20‰), may be difficult to differentiate in environmental systems, where the acetate signal deviates by ±10‰ from the $\delta^{13}C$ value of total organic carbon (65). Part of this variation may originate from the contribution of acetogenically formed ^{13}C-depleted acetate. Indeed, incubations of lake sediments resulted in ^{13}C-depleted acetate only under conditions of H_2/CO_2 addition, not in control experiments with N_2 (66), suggesting that the acetogens in the latter samples either are less active or grow on complex substrates.

TABLE 2 Average fractionation into biomass for different organismic groups and substrates[a]

Organismic group	Substrate	$\Delta_{substrate\text{-}biomass}$ (avg ± SD)	No. of replicates
Acetogens	CO_2	−12.9 ± 5.0	18
Methanogens	CO_2	−18.5 ± 6.3	23
Sulfate reducers	CO_2	−20.4 ± 13.9	5
Phototrophs	CO_2	−23.0 ± 8.4	8
Methanogens	Methanol	−20.5 ± 11.9	5
Methanogens	Acetate	+1.4 ± 6.7	4
Sulfate reducers	Acetate	−6.5 ± 1.3	2
Fermenting bacteria	Glucose	−0.4 ± 1.9	6
Acetogens	Glucose	−3.3 ± 3.0	6

[a] Details can be found in Table S1 in the supplemental material.

Fractionation into biomass. Many studies use published pure culture fractionation factors to deduce the importance of a certain reaction in environmental settings. Most of these fractionation factors have been calculated using a mass balance equation based on the substrate-to-product conversion but neglecting the buildup of biomass. Hence, we aimed to ascertain if this approach is reasonable. Comparison of the fractionations during catabolism and anabolism shows that fractionation into biomass is usually lower than fractionation during catabolism. For example, the fractionation into biomass is roughly one-third of the fractionation into methane for *M. barkeri* grown on H_2/CO_2 (−13.9‰ versus −45.3‰), acetate (−7.3‰ versus −34.4‰), methanol (−31.1‰ versus −83.4‰), or trimethylamine (−24.8‰ versus −66.5‰) (22).

So far, the fractionation of pure bacterial cultures into biomass has been documented mainly using endpoint measurements of the microbial biomass (see Table S1 in the supplemental material). In contrast, we wanted to calculate the apparent fractionation into biomass following a time series experiment. Indeed, we found that the fractionation during anabolism was roughly two-thirds of the fractionation during catabolism. We consider some possible reasons for this ratio in the discussion accompanying Fig. S8 in the supplemental material.

In general, we would conclude that the fractionation into biomass is usually weaker than the fractionation during catabolism. Oxidation of glucose gives a high energy yield ($\Delta G^{o\prime} = -2{,}870$ kJ mol^{-1}), while anaerobic fermentation to CO_2 and CH_4 liberates much less energy ($\Delta G^{o\prime} = -390$ kJ mol^{-1}) (67). Hence, it can be assumed that under anaerobic conditions, most of the available carbon is used for catabolism and only a small portion can be used for anabolism. Therefore, it is unlikely that the bias caused by the fractionation into biomass will have an impact on the apparent fractionation of the catabolic reactions.

Another way to rationalize the fractionation into biomass becomes apparent when we compare different substrates (Table 2). The strongest fractionation can be found for C_1 compounds (CO_2, methanol) ($\Delta_{substrate\text{-}biomass}$, −12.9‰ to −23‰). In comparison, the fractionation into biomass for organisms using acetate is much weaker ($\Delta_{substrate\text{-}biomass}$, 1.4‰ to −6.5‰), while organisms utilizing larger molecules, such as glucose, have almost no discriminatory power with regard to the different carbon isotopes ($\Delta_{substrate\text{-}biomass}$, −0.4‰ to −3.3‰).

The isotope signal of organic carbon in environmental samples is rather constant, as is the signal in important carbon pools (65). Usually, the small differences observed can be explained by the small fractionation factors reported for fermentative processes (catabolic as well as anabolic). On the other hand, strong fractionation into biomass has been reported for methanogens by use of endpoint measurements (22) and has been observed for acetogens grown on H_2/CO_2 (this study). Indeed, our results suggest that the fractionation of autotrophic organisms into their respective biomass is relatively strong and may, in principle, affect the organic carbon pool in environmental samples. However, the microbial communities responsible for, e.g., methanogenesis usually constitute only a small percentage of the total microbial community, and hence, it may be difficult to follow the isotopic differences imparted by C_1 metabolism in environmental settings.

ACKNOWLEDGMENTS

We thank Ralf Conrad (MPI Marburg) for critical reading of the manuscript. We thank three anonymous referees for valuable comments. We thank Rolf Thauer (MPI Marburg) and Wolfgang Buckel (MPI Marburg) for helpful discussions on the isotopic fractionation into biomass.

REFERENCES

1. **Drake HL, Gößner AS, Daniel SL.** 2008. Old acetogens, new light. Ann N Y Acad Sci **1125:**100–128. http://dx.doi.org/10.1196/annals.1419.016.
2. **Drake HL, Kuesel K, Matthies C.** 2002. Ecological consequences of the phylogenetic and physiological diversities of acetogens. Antonie Van Leeuwenhoek **81:**203–213. http://dx.doi.org/10.1023/A:1020514617738.
3. **Drake HL, Küsel K, Matthies C.** 2006. Acetogenic prokaryotes, p 354–420. *In* Dworkin M, Falkow S, Rosenberg E, Schleifer K-H, Stackebrandt E (ed), The prokaryotes: an evolving electronic resource for the microbiological community, 3rd ed, vol 2. Springer, New York, NY.
4. **Berg IA.** 2011. Ecological aspects of the distribution of different autotrophic CO_2 fixation pathways. Appl Environ Microbiol **77:**1925–1936. http://dx.doi.org/10.1128/AEM.02473-10.
5. **Huegler M, Sievert SM.** 2011. Beyond the Calvin cycle: autotrophic carbon fixation in the ocean. Annu Rev Mar Sci **3:**261–289. http://dx.doi.org/10.1146/annurev-marine-120709-142712.
6. **Wood HG.** 1952. A study of carbon dioxide fixation by mass determination of the types of C^{13}-acetate. J Biol Chem **194:**905–931.
7. **Schuchmann K, Muller V.** 2014. Autotrophy at the thermodynamic limit of life: a model for energy conservation in acetogenic bacteria. Nat Rev Microbiol **12:**809–821. http://dx.doi.org/10.1038/nrmicro3365.
8. **Ragsdale SW, Pierce E.** 2008. Acetogenesis and the Wood-Ljungdahl pathway of CO_2 fixation. Biochim Biophys Acta **1784:**1873–1898. http://dx.doi.org/10.1016/j.bbapap.2008.08.012.
9. **Conrad R.** 2005. Quantification of methanogenic pathways using stable carbon isotopic signatures: a review and a proposal. Org Geochem **36:**739–752. http://dx.doi.org/10.1016/j.orggeochem.2004.09.006.
10. **Elsner M, Zwank L, Hunkeler D, Schwarzenbach RP.** 2005. A new concept linking observable stable isotope fractionation to transformation pathways of organic pollutants. Environ Sci Technol **39:**6896–6916. http://dx.doi.org/10.1021/es0504587.
11. **Hayes JM.** 1993. Factors controlling ^{13}C contents of sedimentary organic-compounds—principles and evidence. Mar Geol **113:**111–125. http://dx.doi.org/10.1016/0025-3227(93)90153-M.
12. **Mook WG, Bommerson JC, Staverman WH.** 1974. Carbon isotope fractionation between dissolved bicarbonate and gaseous carbon dioxide. Earth Planet Sci Lett **22:**169–176. http://dx.doi.org/10.1016/0012-821X(74)90078-8.
13. **Myrttinen A, Becker V, Barth J.** 2012. A review of methods used for equilibrium isotope fractionation investigations between dissolved inorganic carbon and CO_2. Earth-Sci Rev **115:**192–199. http://dx.doi.org/10.1016/j.earscirev.2012.08.004.
14. **Northrop DB.** 1981. The expression of isotope effects on enzyme-catalyzed reactions. Annu Rev Biochem **50:**103–131. http://dx.doi.org/10.1146/annurev.bi.50.070181.000535.
15. **Ohkouchi N, Ogawa NO, Chikaraishi Y, Tanaka H, Wada E.** 2015. Biochemical and physiological bases for the use of carbon and nitrogen isotopes in environmental and ecological studies. Prog Earth Planet Sci **2:**2–17. http://dx.doi.org/10.1186/s40645-014-0031-4.
16. **Wing BA, Halevy I.** 2014. Intracellular metabolite levels shape sulfur isotope fractionation during microbial sulfate respiration. Proc Natl Acad Sci U S A **111:**18116–18125. http://dx.doi.org/10.1073/pnas.1407502111.
17. **Mariotti A, Germon JC, Hubert P, Kaiser P, Letolle R, Tardieux A, Tardieux P.** 1981. Experimental determination of nitrogen kinetic isotope fractionation: some principles; illustration for the denitrification and nitrification processes. Plant Soil **62:**413–430. http://dx.doi.org/10.1007/BF02374138.
18. **Botz R, Pokojski HD, Schmitt M, Thomm M.** 1996. Carbon isotope fractionation during bacterial methanogenesis by CO_2 reduction. Org Geochem **25:**255–262. http://dx.doi.org/10.1016/S0146-6380(96)00129-5.
19. **Games LM, Hayes JM, Gunsalus P.** 1978. Methane-producing bacteria: natural fractionations of the stable carbon isotopes. Geochim Cosmochim Acta **42:**1295–1297. http://dx.doi.org/10.1016/0016-7037(78)90123-0.
20. **Penning H, Plugge CM, Galand PE, Conrad R.** 2005. Variation of carbon isotope fractionation in hydrogenotrophic methanogenic microbial cultures and environmental samples at different energy status. Global Change Biol **11:**2103–2113. http://dx.doi.org/10.1111/j.1365-2486.2005.01076.x.
21. **Valentine DL, Chidthaisong A, Rice A, Reeburgh WS, Tyler SC.** 2004. Carbon and hydrogen isotope fractionation by moderately thermophilic methanogens. Geochim Cosmochim Acta **68:**1571–1590. http://dx.doi.org/10.1016/j.gca.2003.10.012.
22. **Londry KL, Dawson KG, Grover HD, Summons RE, Bradley AS.** 2008. Stable carbon isotope fractionation between substrates and products of *Methanosarcina barkeri*. Org Geochem **39:**608–621. http://dx.doi.org/10.1016/j.orggeochem.2008.03.002.
23. **Penger J, Conrad R, Blaser M.** 2012. Stable carbon isotope fractionation by methylotrophic methanogenic archaea. Appl Environ Microbiol **78:**7596–7602. http://dx.doi.org/10.1128/AEM.01773-12.
24. **Gelwicks JT, Risatti JB, Hayes JM.** 1994. Carbon isotope effects associated with aceticlastic methanogenesis. Appl Environ Microbiol **60:**467–472.
25. **Goevert D, Conrad R.** 2009. Effect of substrate concentration on carbon isotope fractionation during acetoclastic methanogenesis by *Methanosarcina barkeri* and *M. acetivorans* and in rice field soil. Appl Environ Microbiol **75:**2605–2612. http://dx.doi.org/10.1128/AEM.02680-08.
26. **House CH, Schopf JW, Stetter KO.** 2003. Carbon isotopic fractionation by Archaeans and other thermophilic prokaryotes. Org Geochem **34:**345–356. http://dx.doi.org/10.1016/S0146-6380(02)00237-1.
27. **Penning H, Claus P, Casper P, Conrad R.** 2006. Carbon isotope fractionation during acetoclastic methanogenesis by *Methanosaeta concilii* in culture and a lake sediment. Appl Environ Microbiol **72:**5648–5652. http://dx.doi.org/10.1128/AEM.00727-06.
28. **Conrad R, Claus P, Casper P.** 2010. Stable isotope fractionation during the methanogenic degradation of organic matter in the sediment of an acidic bog lake, Lake Grosse Fuchskuhle. Limnol Oceanogr **55:**1932–1942. http://dx.doi.org/10.4319/lo.2010.55.5.1932.
29. **Conrad R, Ji Y, Noll M, Klose M, Claus P, Enrich-Prast A.** 2014. Response of the methanogenic microbial communities in Amazonian oxbow lake sediments to desiccation stress. Environ Microbiol **16:**1682–1694. http://dx.doi.org/10.1111/1462-2920.12267.
30. **Conrad R, Klose M, Claus P, Enrich-Prast A.** 2010. Methanogenic pathway, ^{13}C isotope fractionation, and archaeal community composition in the sediment of two clear-water lakes of Amazonia. Limnol Oceanogr **55:**689–702. http://dx.doi.org/10.4319/lo.2009.55.2.0689.
31. **Conrad R, Klose M, Lu Y, Chidthaisong A.** 2012. Methanogenic pathway and archaeal communities in three different anoxic soils amended with rice straw and maize straw. Front Microbiol **3:**4. http://dx.doi.org/10.3389/fmicb.2012.00004.
32. **Daebeler A, Gansen M, Frenzel P.** 2013. Methyl fluoride affects methanogenesis rather than community composition of methanogenic archaea in a rice field soil. PLoS One **8:**e53656. http://dx.doi.org/10.1371/journal.pone.0053656.
33. **Janssen PH, Frenzel P.** 1997. Inhibition of methanogenesis by methyl fluoride: studies of pure and defined mixed cultures of anaerobic bacteria and archaea. Appl Environ Microbiol **63:**4552–4557.
34. **Blaser MB, Dreisbach LK, Conrad R.** 2013. Carbon isotope fractionation of 11 acetogenic strains grown on H_2 and CO_2. Appl Environ Microbiol **79:**1787–1794. http://dx.doi.org/10.1128/AEM.03203-12.
35. **Gelwicks JT, Risatti JB, Hayes JM.** 1989. Carbon isotope effects associ-

ated with autotrophic acetogenesis. Org Geochem **14:**441–446. http://dx.doi.org/10.1016/0146-6380(89)90009-0.
36. **Preuss A, Schauder R, Fuchs G, Stichler W.** 1989. Carbon isotope fractionation by autotrophic bacteria with 3 different CO_2 fixation pathways. Z Naturforsch C **44:**397–402.
37. **Blair N, Leu A, Munoz E, Olsen J, Kwong E, Des Marais DJ.** 1985. Carbon isotopic fractionation in heterotrophic microbial-metabolism. Appl Environ Microbiol **50:**996–1001.
38. **Botsch KC, Conrad R.** 2011. Fractionation of stable carbon isotopes during anaerobic production and degradation of propionate in defined microbial cultures. Org Geochem **42:**289–295. http://dx.doi.org/10.1016/j.orggeochem.2011.01.005.
39. **Penning H, Conrad R.** 2006. Carbon isotope effects associated with mixed-acid fermentation of saccharides by *Clostridium papyrosolvens*. Geochim Cosmochim Acta **70:**2283–2297. http://dx.doi.org/10.1016/j.gca.2006.01.017.
40. **Zhang CLL, Ye Q, Reysenbach AL, Gotz D, Peacock A, White DC, Horita J, Cole DR, Fong J, Pratt L, Fang JS, Huang YS.** 2002. Carbon isotopic fractionations associated with thermophilic bacteria *Thermotoga maritima* and *Persephonella marina*. Environ Microbiol **4:**58–64. http://dx.doi.org/10.1046/j.1462-2920.2002.00266.x.
41. **Ljungdahl LG, Andreesen JR.** 1978. Formate dehydrogenase, a selenium-tungsten enzyme from *Clostridium thermoaceticum*. Methods Enzymol **53:**360–372. http://dx.doi.org/10.1016/S0076-6879(78)53042-5.
42. **Ragsdale SW.** 2008. Enzymology of the Wood-Ljungdahl pathway of acetogenesis. Ann N Y Acad Sci **1125:**129–136. http://dx.doi.org/10.1196/annals.1419.015.
43. **Fontaine FE, Peterson WH, McCoy E, Johnson MJ, Ritter GJ.** 1942. A new type of glucose fermentation by *Clostridium thermoaceticum* n.sp. J Bacteriol **43:**701–715.
44. **Fröstl JM, Seifritz C, Drake HL.** 1996. Effect of nitrate on the autotrophic metabolism of the acetogens *Clostridium thermoautotrophicum* and *Clostridium thermoaceticum*. J Bacteriol **178:**4597–4603.
45. **Arendsen AF, Soliman MQ, Ragsdale SW.** 1999. Nitrate-dependent regulation of acetate biosynthesis and nitrate respiration by *Clostridium thermoaceticum*. J Bacteriol **181:**1489–1495.
46. **Seifritz C, Daniel SL, Gossner A, Drake HL.** 1993. Nitrate as a preferred electron sink for the acetogen *Clostridium thermoaceticum*. J Bacteriol **175:**8008–8013.
47. **Pearson A.** 2010. Pathways of carbon assimilation and their impact on organic matter values $\delta^{13}C$, p 143–156. *In* Timmis KN (ed), Handbook of hydrocarbon and lipid microbiology. Springer, Berlin, Germany.
48. **Zyakun AM, Kochetkov VV, Baskunov BP, Zakharchenko VN, Peshenko VP, Laurinavichius KS, Anokhina TO, Siunova TV, Sizova OI, Boronin AM.** 2013. Use of glucose and carbon isotope fractionation by microbial cells immobilized on solid-phase surface. Microbiology **82:**280–289. http://dx.doi.org/10.1134/S0026261713030156.
49. **Hunkeler D, Aravena R.** 2000. Evidence of substantial carbon isotope fractionation among substrate, inorganic carbon, and biomass during aerobic mineralization of 1,2-dichloroethane by *Xanthobacter autotrophicus*. Appl Environ Microbiol **66:**4870–4876. http://dx.doi.org/10.1128/AEM.66.11.4870-4876.2000.
50. **Wolin EA, Wolin MJ, Wolfe RS.** 1963. Formation of methane by bacterial extracts. J Biol Chem **238:**2882–2886.
51. **Brand WA.** 1996. High precision isotope ratio monitoring techniques in mass spectrometry. J Mass Spectrom **31:**225–235. http://dx.doi.org/10.1002/(SICI)1096-9888(199603)31:3<225::AID-JMS319>3.0.CO;2-L.
52. **Krummen M, Hilkert AW, Juchelka D, Duhr A, Schluter HJ, Pesch R.** 2004. A new concept for isotope ratio monitoring liquid chromatography/mass spectrometry. Rapid Commun Mass Spectrom **18:**2260–2266. http://dx.doi.org/10.1002/rcm.1620.
53. **Hayes JM.** 2 August 2002, revision date. Practice and principles of isotopic measurements in organic geochemistry. http://web.gps.caltech.edu/~als/research_articles/other_stuff/hayespnp.pdf.
54. **Hayes JM.** 2004. Isotopic order, biogeochemical processes, and earth history: Goldschmidt lecture, Davos, Switzerland, August 2002. Geochim Cosmochim Acta **68:**1691–1700. http://dx.doi.org/10.1016/j.gca.2003.10.023.
55. **O'Leary MH.** 1981. Carbon isotope fractionation in plants. Phytochemistry **20:**553–567. http://dx.doi.org/10.1016/0031-9422(81)85134-5.
56. **Bowling DR, Pataki DE, Randerson JT.** 2008. Carbon isotopes in terrestrial ecosystem pools and CO_2 fluxes. New Phytol **178:**24–40. http://dx.doi.org/10.1111/j.1469-8137.2007.02342.x.
57. **Schoeller DA, Klein PD, Watkins JB, Heim T, MacLean WC, Jr.** 1980. ^{13}C abundances of nutrients and the effect of variations in ^{13}C isotopic abundances of test meals formulated for $^{13}CO_2$ breath tests. Am J Clin Nutr **33:**2375–2385.
58. **Krzycki JA, Kenealy WR, Deniro MJ, Zeikus JG.** 1987. Stable carbon isotope fractionation by *Methanosarcina barkeri* during methanogenesis from acetate, methanol, or carbon dioxide-hydrogen. Appl Environ Microbiol **53:**2597–2599.
59. **Sim MS, Ono S, Donovan K, Templer SP, Bosak T.** 2011. Effect of electron donors on the fractionation of sulfur isotopes by a marine *Desulfovibrio* sp. Geochim Cosmochim Acta **75:**4244–4259. http://dx.doi.org/10.1016/j.gca.2011.05.021.
60. **Ono S, Sim MS, Bosak T.** 2014. Predictive isotope model connects microbes in culture and nature. Proc Natl Acad Sci U S A **111:**18102–18103. http://dx.doi.org/10.1073/pnas.1420670111.
61. **Blaser MB, Dreisbach LK, Conrad R.** 2015. Carbon isotope fractionation of *Thermoanaerobacter kivui* in different growth media and at different total inorganic carbon concentration. Org Geochem **81:**45–52. http://dx.doi.org/10.1016/j.orggeochem.2015.01.013.
62. **van der Meijden P, van der Drift C, Vogels GD.** 1984. Methanol conversion in *Eubacterium limosum*. Arch Microbiol **138:**360–364. http://dx.doi.org/10.1007/BF00410904.
63. **Hattori S.** 2008. Syntrophic acetate-oxidizing microbes in methanogenic environments. Microbes Environ **23:**118–127. http://dx.doi.org/10.1264/jsme2.23.118.
64. **Hattori S, Kamagata Y, Hanada S, Shoun H.** 2000. *Thermacetogenium phaeum* gen. nov., sp. nov., a strictly anaerobic, thermophilic, syntrophic acetate-oxidizing bacterium. Int J Syst Evol Microbiol **50:**1601–1609. http://dx.doi.org/10.1099/00207713-50-4-1601.
65. **Conrad R, Claus P, Chidthaisong A, Lu Y, Fernandez Scavino A, Liu Y, Angel R, Galand PE, Casper P, Guerin F, Enrich-Prast A.** 2014. Stable carbon isotope biogeochemistry of propionate and acetate in methanogenic soils and lake sediments. Org Geochem **73:**1–7. http://dx.doi.org/10.1016/j.orggeochem.2014.03.010.
66. **Heuer VB, Krueger M, Elvert M, Hinrichs KU.** 2010. Experimental studies on the stable carbon isotope biogeochemistry of acetate in lake sediments. Org Geochem **41:**22–30. http://dx.doi.org/10.1016/j.orggeochem.2009.07.004.
67. **Schink B.** 1997. Energetics of syntrophic cooperation in methanogenic degradation. Microbiol Mol Biol Rev **61:**262–280.